Supporting Information

Mixed lead carboxylates relevant to soap formation in oil and tempera paintings: the study of the crystal structure by complementary XRPD and ssNMR

Eva Kočí[a], Jan Rohlíček[b], Libor Kobera[c], Jiří Plocek[a], Silvie Švarcová[a]*and Petr Bezdička[a]

[a]Institute of Inorganic Chemistry of the Czech Academy of Sciences, ALMA Laboratory, Husinec-Řež 1001, 250 68 Husinec-Řež, Czech Republic
[b]Institute of Physics of the Czech Academy of Sciences, Na Slovance 1999/2, 182 21 Prague 8, Czech Republic
[c]Institute of Macromolecur Chemistry of the Czech Academy of Sciences, Heyrovského nám. 2, 162 06 Praha 6, Czech Republic

e-mails: koci@iic.cas.cz, bezdicka@iic.cas.cz, rohlicek@fzu.cz, kobera@imc.cas.cz, plocek@iic.cas.cz, svarcova@iic.cas.cz,

*corresponding author: e-mail: svarcova@iic.cas.cz, phone number: +420 311 236 937

Table of contents:

Measurement details of elemental analysis

Elemental analysis (EA) was performed in the following analyzer: Thermo Scientific FlashSmart^{TM} 2000 Elemental analyzer (United States). The combustion tube packing was supplied with the instrument and consisted of the following components: EA-2000 chromium oxidizer, high quality copper reducer, and silver cobaltous-cobaltic oxide. Samples were weighed on a balance Mettler Toledo; model: WXTE (Switzerland). All the determinations were done in triples.

Analysis of the sample; portions of samples with a mass around 1 mg were weighed in tin containers together with a vanadium pentoxide (10 mg). Then samples were packed thoroughly and placed in the automated sampler, from which they were transferred to the oxidation tube at regular intervals. A sample was burned in a vertical reactor (oxidation tube) in the dynamic mode (at 950 °C) in an He flow (140 mL/min) with the addition of O_2 (21 mL) at the instant of sample introduction. After the pyrolysis, the resulting products were after oxidized in the lower part of the reactor filled with a catalytic oxide composition and then passed through the reduction zone, as mentioned above. Resulting N_2, CO_2, and H_2O were separated on a multiseparation column (PTFE; 2 m; 6x5 mm) heated to 75 °C and determined with a thermal conductivity detector. The overall run time of one sample was about 480 seconds. The concentration of each element in the EA analyzer was calculated after the measurement of the corresponding peak areas in the chromatogram.

XRPD measurement of model tempera paint

The sample of model tempera paint was measured using a PANalytical X ´Pert PRO diffractometer equipped with a conventional X-ray tube ($Co_{K\alpha}$ 40 kV, 30 mA, line focus) and a multichannel detector X'Celerator with an anti-scatter shield. X-ray patterns were measured in the range of 1 to 40° 2Θ with a step of 0.0167° and 200 s counting per step. Bragg-Brentano setting was used with 0.02 rad Soller slit, 0.0625° divergence slit, 0.125° anti-scatter slit, and 15 mm mask in the incident beam, 5.0 mm anti-scatter slit, 0.02 rad Soller slit and Fe beta-filter in the diffracted beam.

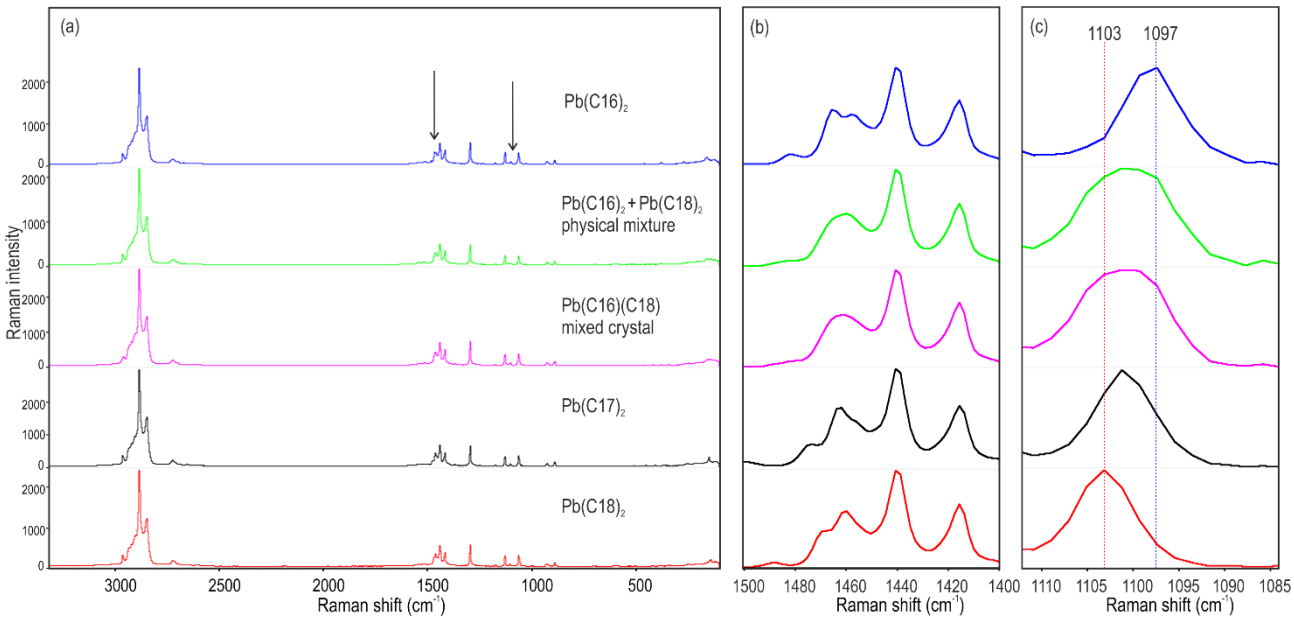

Fig. S1 Raman spectra of selected single and mixed lead carboxylates (a). Arrows mark bands differing in particular carboxylates. Details of spectra displaying bands attributed to CH_2 bending (b) and C-C stretching (c) vibrations where some differences can be observed. Dotted lines mark positions of maxima of bands of C-C stretching for lead stearate (red) and lead palmitate (blue).

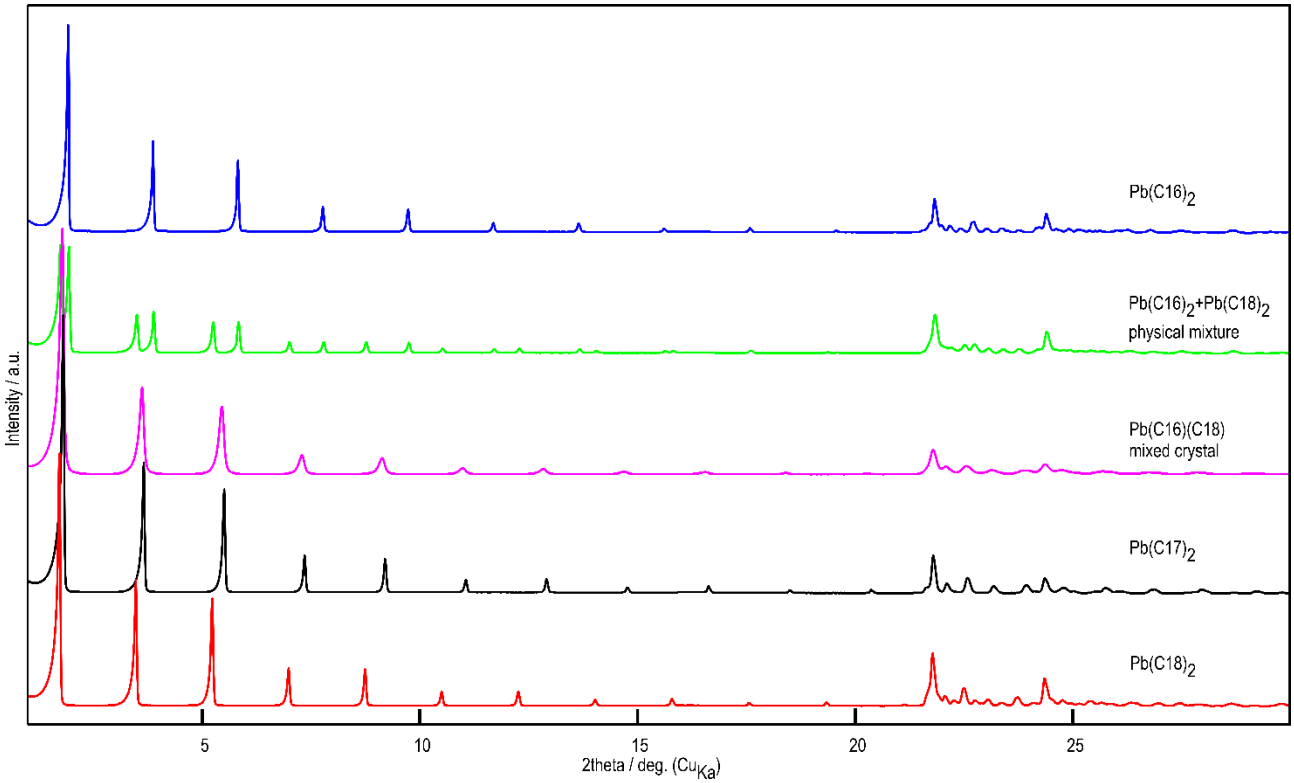

Fig. S2 XRPD patterns of selected single and mixed lead carboxylates illustrating the possibility to distinguish mixed crystal and physical mixture of corresponding composition.

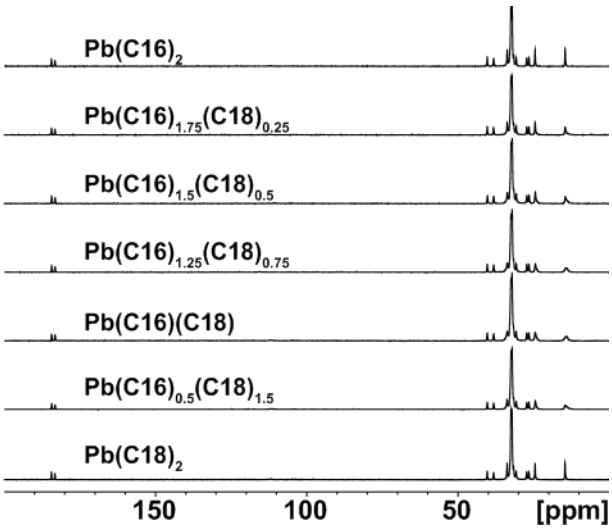

Fig. S3 Experimental full-range ^{13}C CP/MAS NMR spectra of simple and mixed lead-carboxylates acquired at 10 kHz using 11.7 T spectrometer.

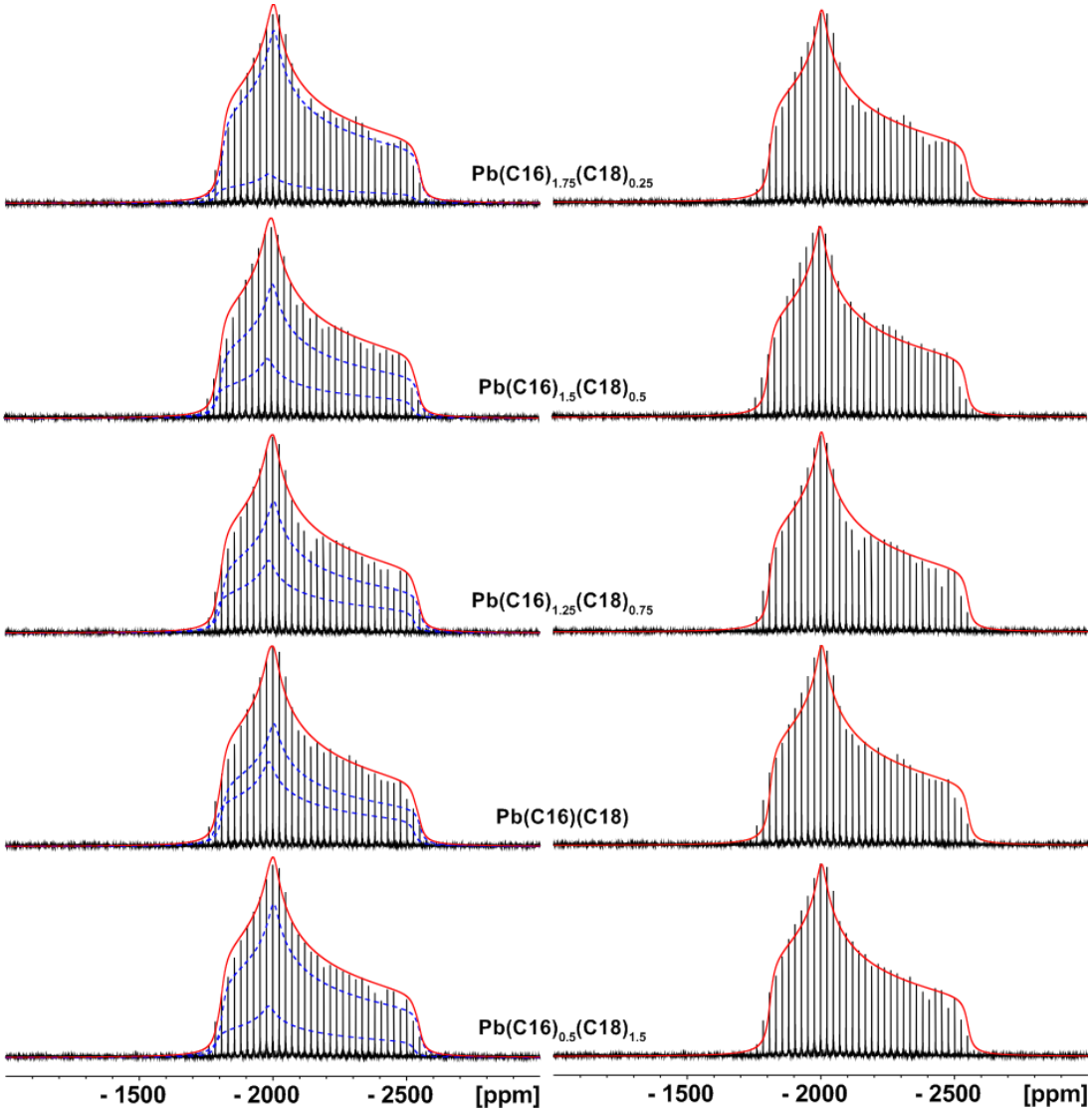

Fig. S4 The comparison of simulated spectral lines for experimental ^{207}Pb WURST-QCPMG NMR spectra (black solid line) of mixed lead-carboxylates. Column on the left - simulations using two spectral lines (blue dashed lines) and their sums (red solid line). Column on the right - simulations using single spectral line (red solid line).

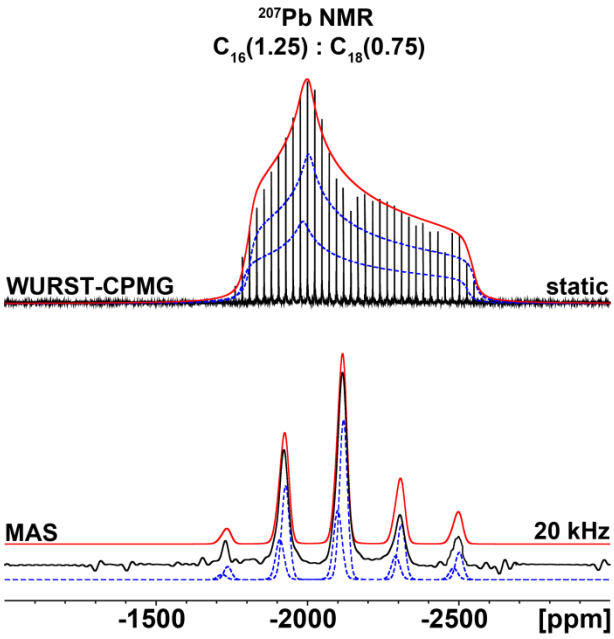

Fig. S5 Comparison of experimental ^{207}Pb MAS and ^{207}Pb WURST-CPMG NMR spectra (black solid line), simulations for the two independent lead atoms (blue dashed lines) and their sums (red solid line) of the selected mixed lead-carboxylate.

Description of the Rietveld refinement

Rietveld refinement of lead carboxylates was performed in JANA2006 software.[1] For all the crystal structures of prepared mixed lead-carboxylates the initial model was taken from the crystal structure of $Pb(C18)_2$ (CSD's ref. code PAXPIQ) [2] and the refinement procedure was identical for all samples.

Occupancies of the ethyl groups at the end of both independent aliphatic C18 chains were refined to simulate possible substitutional disorder of C18 and C16. To keep a reasonable geometry of the molecular model all bonds (Pb-O, C-O and C-C) together with its bond-angles and torsion angles between carbon atoms in aliphatic chains had to be restrained according to the crystal structure of $Pb(C18)_2$. To keep a reasonable geometry of the molecular model all bonds (Pb-O, C-O and C-C; s.u. of Pb-O distances were set to 0.005 and of C-O and C-C 0.001) together with its bond-angles (s.u. for O-Pb-O was 0.02 and for other 0.01) and torsion angles between carbon atoms in aliphatic chains (with s.u. of 1) had to be restrained according to the crystal structure of $Pb(C18)_2$. Torsion angles between carbon atoms of both ending ethylene groups were not applied to allow possible larger movement of the disordered ends of aliphatic chains. Bond distances were kept very strictly, but torsion angles were applied only very roughly allowing a distortion of the aliphatic chains but restricting violation of the zigzag atomic arrangement in the chain. ADP parameter of lead atom was freely refined as harmonic, but in the case of carbon and oxygen atoms, one shared isotropic ADP parameter was used and all hydrogen atoms were kept in positions calculated from geometry.

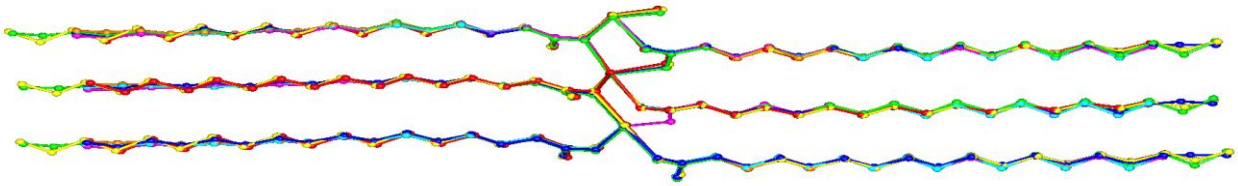

Fig. S6 Overlaying of mixed lead carboxylates $Pb(C16)_{2-x}(C18)_x$ (model 2) with pure $Pb(C18)_2$ and $Pb(C16)_2$. Disordered parts with occupancy lower than 0.5 are not displayed.

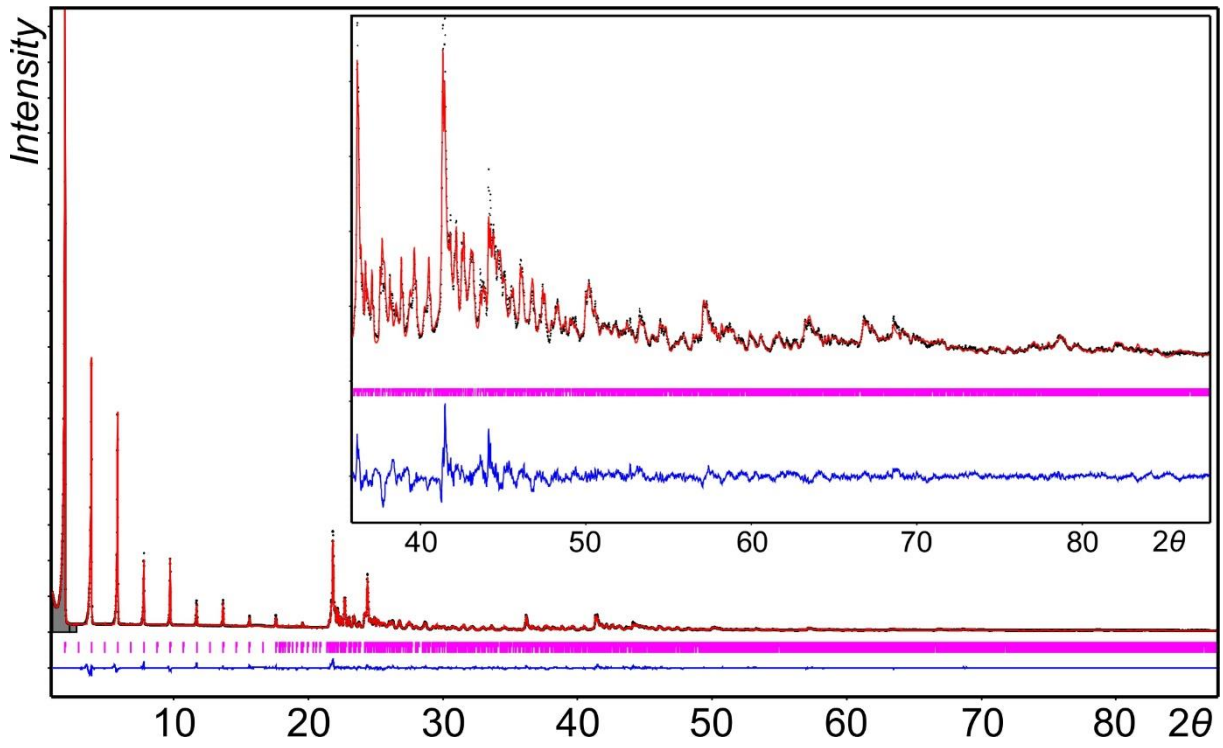

Fig. S7 Final Rietveld plot of the XRPD of $Pb(C16)_2$. Black dots – measured data, red curve – calculated profile, blue curve – difference between measured and calculated profile and magenta vertical bars are positions of Bragg's reflections.

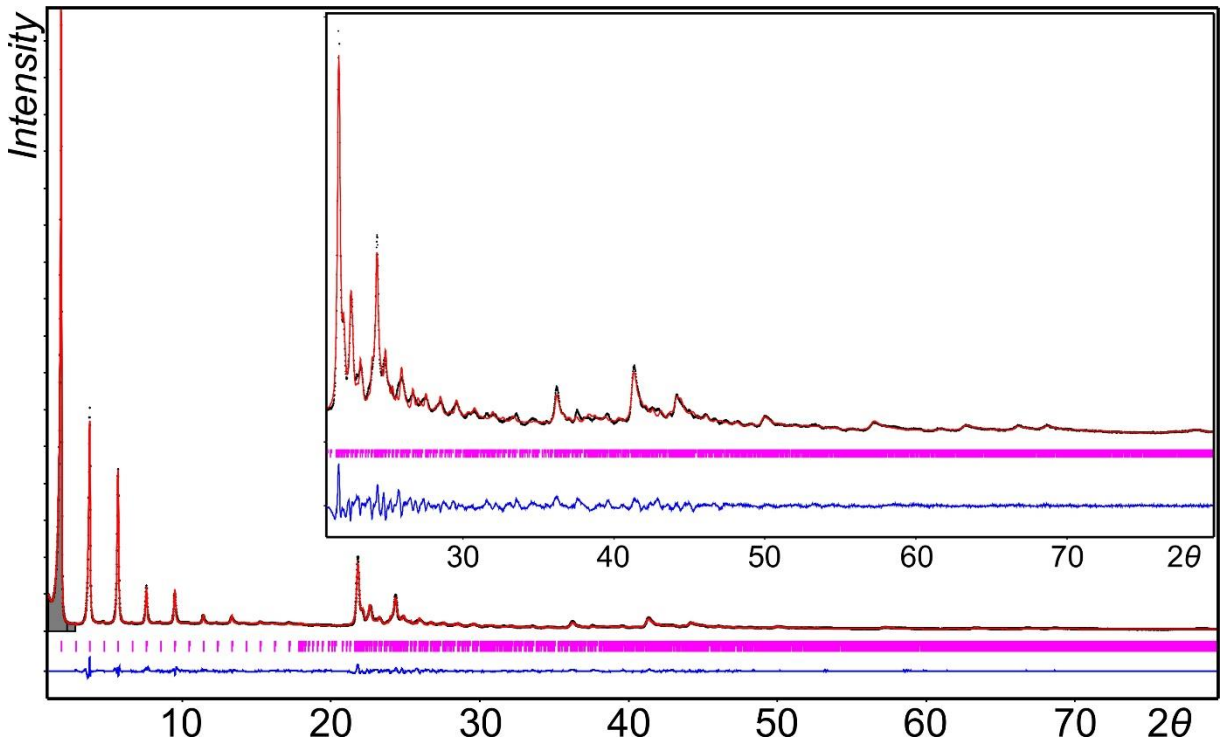

Fig. S8 Final Rietveld plot of the XRPD of $Pb(C16)_{1.75}(C18)_{0.25}$. Black dots – measured data, red curve – calculated profile, blue curve – difference between measured and calculated profile and magenta vertical bars are positions of Bragg's reflections.

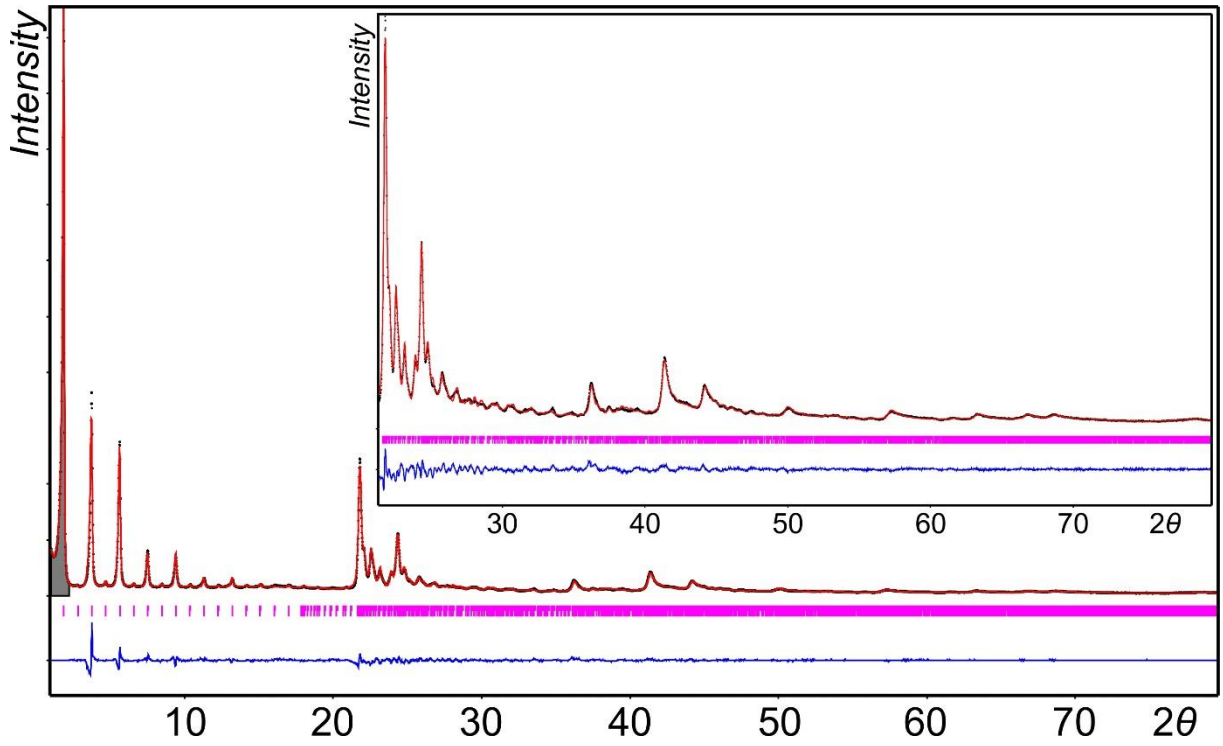

Fig. S9 Final Rietveld plot of the XRPD of $Pb(C16)_{1.5}(C18)_{0.5}$. Black dots – measured data, red curve – calculated profile, blue curve – difference between measured and calculated profile and magenta vertical bars are positions of Bragg's reflections.

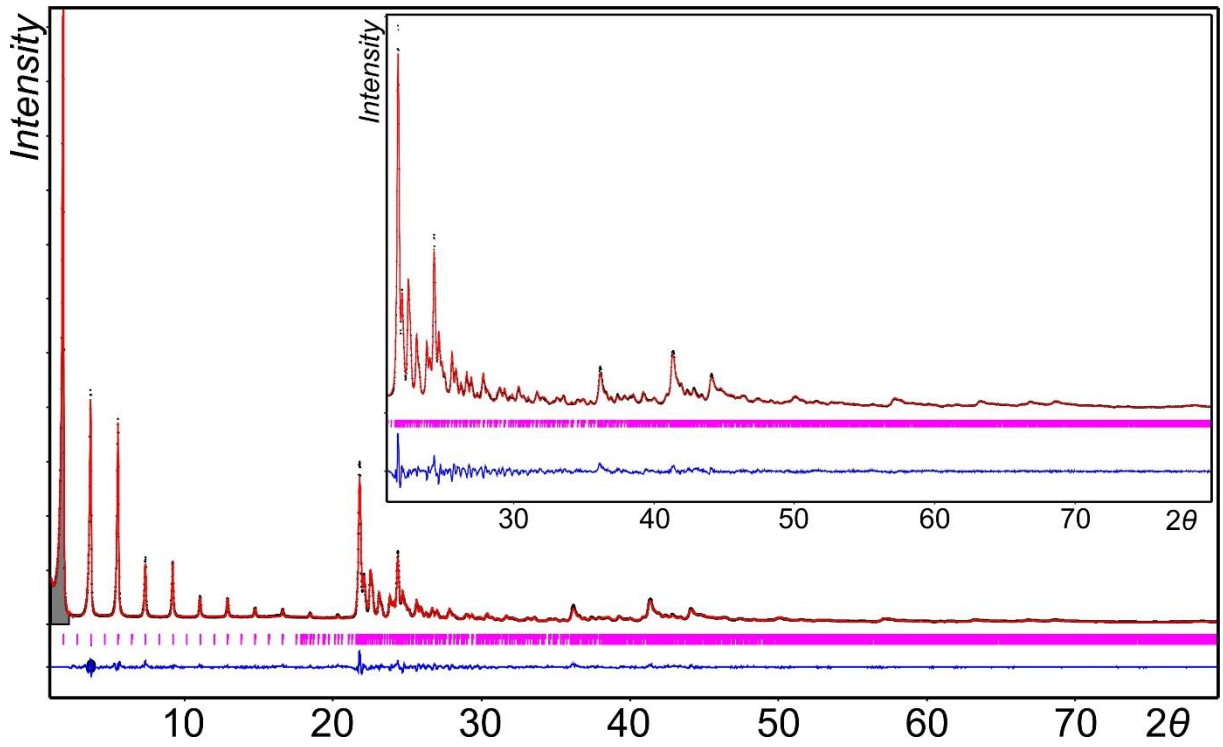

Fig. S10 Final Rietveld plot of the XRPD of $Pb(C16)_{1.25}(C18)_{0.75}$. Black dots – measured data, red curve – calculated profile, blue curve – difference between measured and calculated profile and magenta vertical bars are positions of Bragg's reflections.

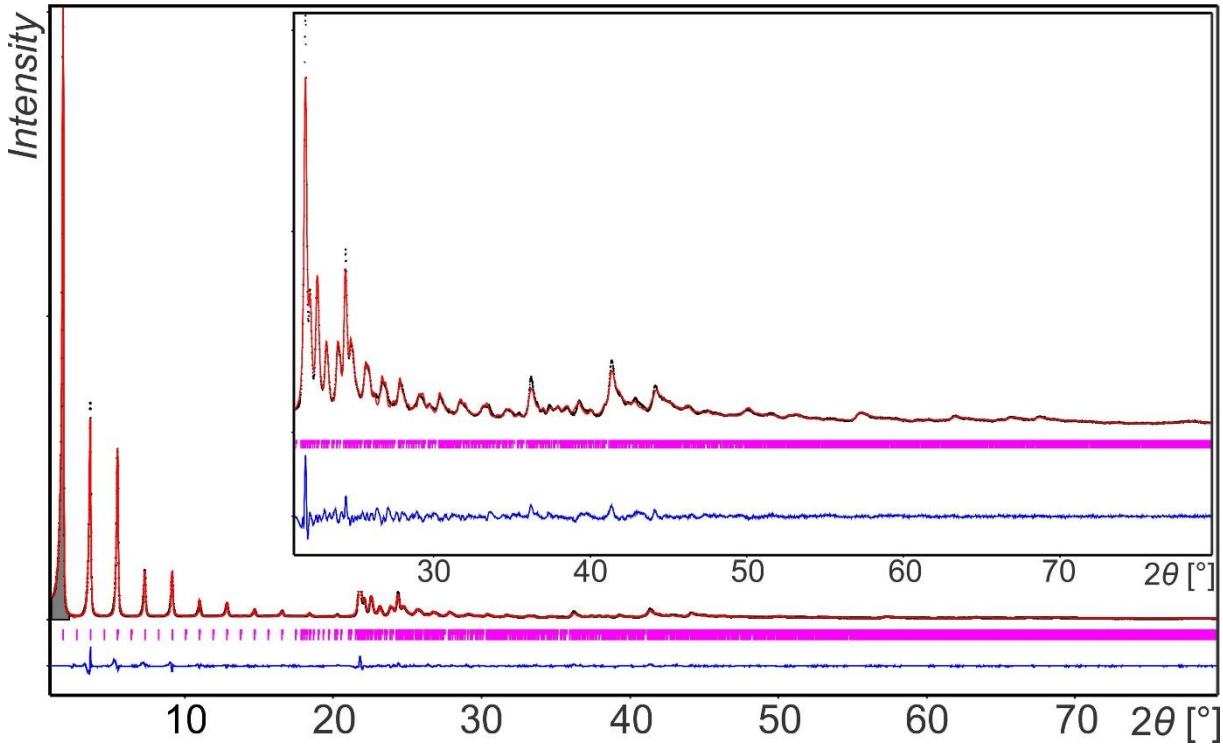

Fig. S11 Final Rietveld plot of the XRPD of Pb(C16)(C18). Black dots – measured data, red curve – calculated profile, blue curve – difference between measured and calculated profile and magenta vertical bars are positions of Bragg's reflections.

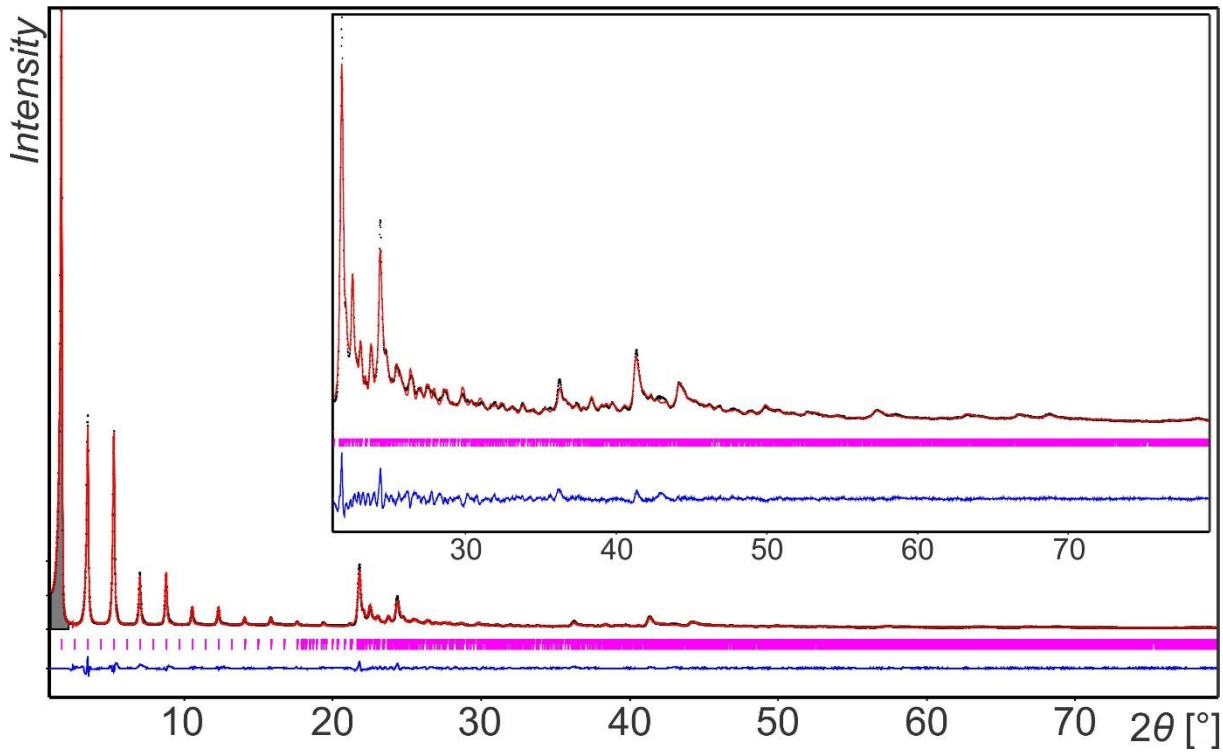

Fig. S12 Final Rietveld plot of the XRPD of $Pb(C16)_{0.5}(C18)_{1.5}$. Black dots – measured data, red curve – calculated profile, blue curve – difference between measured and calculated profile and magenta vertical bars are positions of Bragg's reflections.

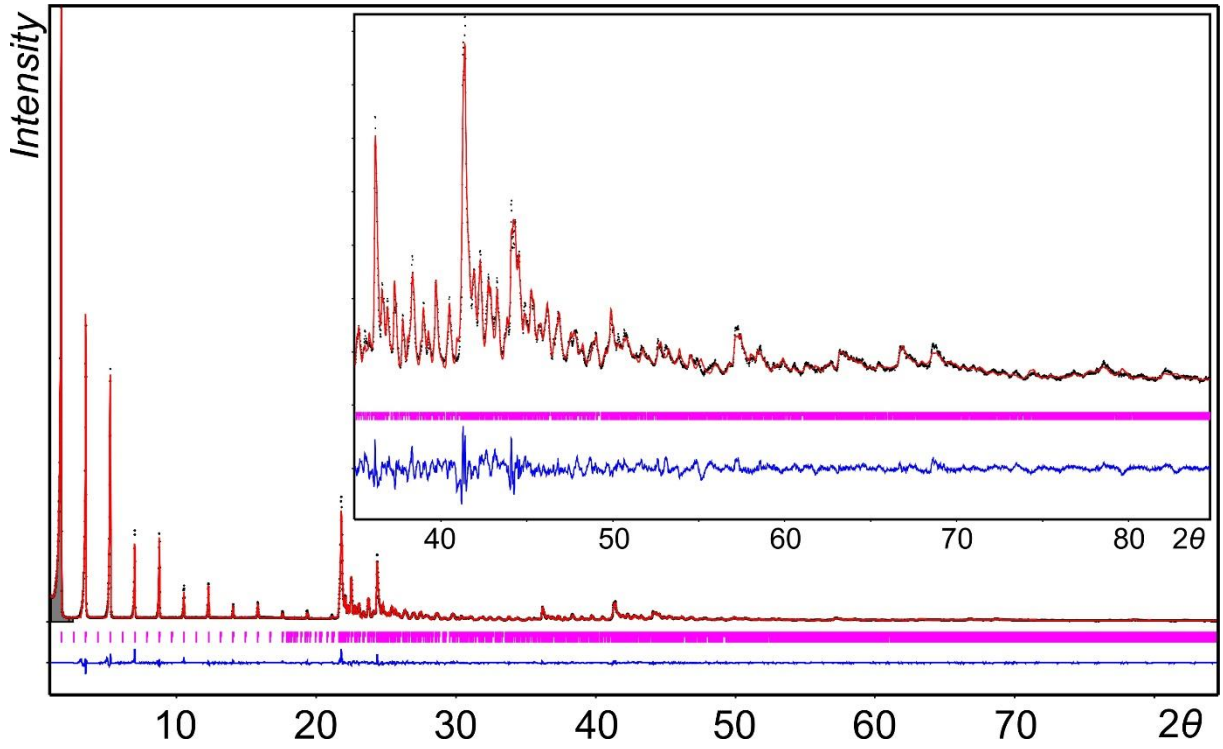

Fig. S13 Final Rietveld plot of the XRPD of $Pb(C_{18})_2$. Black dots – measured data, red curve – calculated profile, blue curve – difference between measured and calculated profile and magenta vertical bars are positions of Bragg's reflections.

Determination of fatty acids in linseed oil by GC-FID analysis

The fatty acid profile of the linseed oil used for model tempera paint was analysed by gas chromatography with flame ionisation detector (GC-FID) according to a certified procedure in the Metrological and Testing Laboratory of University of Chemistry and Technology Prague (Testing laboratory 1316.2 accredited by the CAI according to the EN ISO/IEC 17025:2005). The determined fatty acids are given in Table S1.

Table S1 Fatty acid composition of poppy seed oil (weight %)

Fatty acid*	(%)
Palmitic (C16:0)	4.71
Stearic (C18:0)	3.17
Vaccenic (c18:1n11c)	0.97
Oleic (C18:1n9c)	13.65
Linoleic (C18:2n6c)	16.13
α-linolenic (C18:3n3)	54.75
γ-linolenic (C18:3n6)	0.18
Arachidic (C20:0	0.13
Behenic (C22:0)	0.13

*The acids of concentration under detection limits (i.e., < 0,1% wt.) are not listed.

Calculation of the ratio of C16:C18 in the binder

The ratios of palmitic (hexadecenoic) and stearic (octadecanoic) acids in binders used for model tempera paints were calculated from their weight fractions:

$$w_{C16}(EB) = \frac{w_{EYL}(EY) \cdot w_{C16}(EYL) \cdot m_{EY} + w_{C16}(O) \cdot m_O}{m_{EY} + m_O} \qquad \text{(eq. 1)}$$

$$w_{C18}(EB) = \frac{w_{EYL}(EY) \cdot w_{C18}(EYL) \cdot m_{EY} + w_{C18}(O) \cdot m_O}{m_{EY} + m_O} \qquad \text{(eq. 2)}$$

$w_{C16}(EB)$ weight fraction of palmitic acid in emulsion binder
$w_{C18}(EB)$ weight fraction of stearic acid in emulsion binder
$w_{EYL}(EY)$ weight fraction of egg yolk lipids in egg yolk
$w_{C16}(EYL)$ weight fraction of palmitic acid in egg yolk lipids
$w_{C18}(EYL)$ weight fraction of stearic acid in egg yolk lipids
$w_{C16}(O)$ weight fraction of palmitic acid in oil
$w_{C18}(O)$ weight fraction of stearic acid in oil
m_{EY} mass of egg yolk in binder
m_O mass of oil in binder

$w_{EYL}(EY) = 0.31$*
$w_{C16}(EY) = 0.263$*
$w_{C18}(EY) = 9.2$*
$w_{C16}(O) = 0.472$
$w_{C18}(O) = 0.317$
$m_{EY} = 1$ g
$m_O = 1$ g

*values according to ref. 3 and 4

References

1 V. Petríček, M. Dušek and L. Palatinus, *Zeitschrift fur Krist.*, 2014, **229**, 345–352.

2 F. J. Martínez-Casado, M. Ramos-Riesco, J. A. Rodríguez-Cheda, M. I. Redondo-Yélamos, L. Garrido, A. Fernández-Martínez, J. García-Barriocanal, I. Da Silva, M. Durán-Olivencia and A. Poulain, *Phys. Chem. Chem. Phys.*, 2017, **19**, 17009–17018.

3 L. R. Juneja, in *Hen Eggs*, eds. T. Yamamoto, L. R. Juneja, H. Hatta and M. Kim, CRC Press LLC, 1997, pp. 73–98.

4 H. Sugino, T. Nitoda and L. R. Juneja, in *Hen Eggs*, eds. T. Yamamoto, L. R. Juneja, H. Hatta and M. Kim, 1997.